



**US Army Corps
of Engineers®**
Engineer Research and
Development Center

Multi-Sensor Systems Development for UXO Detection and Discrimination

Hand-Held Dual Magnetic/Electromagnetic Induction Sensor

David Wright, Hollis H. Bennett, Jr., Linda Peyman Dove,
and Dwain K. Butler

April 2008

Multi-Sensor Systems Development for UXO Detection and Discrimination

Hand-Held Dual Magnetic/Electromagnetic Induction Sensor

David Wright

*AETC Incorporated
120 Quade Drive
Cary, NC 27513-7400*

Hollis H. Bennett, Jr., Linda Peyman Dove

*Environmental Laboratory
U.S. Army Engineer Research and Development Center
3909 Halls Ferry Road
Vicksburg, MS 39180-6199*

Dwain K. Butler

*Alion Science and Technology Corporation
U.S. Army Engineer Research and Development Center
3909 Halls Ferry Road
Vicksburg, MS 39180-6199*

Final report

Approved for public release; distribution is unlimited.

Prepared for U.S. Army Corps of Engineers
Washington, DC 20314-1000

Under Restoration Requirement A (1.6.a) UXO Screening,
Detection, and Discrimination

Abstract: The U.S. Army Engineer Research and Development Center (ERDC) in Vicksburg, MS, developed, tested, and demonstrated an innovative, hand-held, dual-sensor unexploded ordnance (UXO) detection and discrimination system. This breakthrough technology markedly reduces UXO false alarm rates by fusing two heretofore incompatible sensor platforms, integrating highly accurate spatial data in real time, and applying advanced modeling and analysis to the co-registered data stream. The ArcSecond® laser positioning module simultaneously integrates co-registered magnetometry and electromagnetic induction (EMI) sensor data with latitude, longitude, and elevation data at the centimeter level. This enables a vast improvement in object detection and classification in the field under a wide variety of complex geological and environmental site conditions and at sites with multiple types of military munitions. Sensor co-registration further enables major advances in physics-based modeling capabilities and applications that are unique for magnetometry and EMI sensor response. Co-registered sensors permitted the application of cooperative and joint inversion techniques that simultaneously solve both the magnetic and EM inverse problem. This approach is considerably more efficient and elegant than inverting each measurement set individually and exclusively. This breakthrough will permit the UXO remediation community to detect and discriminate 90 percent of UXO under complex site conditions, and will lead to an enormous reduction in UXO cleanup costs nationwide.

DISCLAIMER: The contents of this report are not to be used for advertising, publication, or promotional purposes. Citation of trade names does not constitute an official endorsement or approval of the use of such commercial products. All product names and trademarks cited are the property of their respective owners. The findings of this report are not to be construed as an official Department of the Army position unless so designated by other authorized documents.

DESTROY THIS REPORT WHEN NO LONGER NEEDED. DO NOT RETURN IT TO THE ORIGINATOR.

Contents

Figures and Table.....	iv
Preface.....	vi
1 Introduction.....	1
Background	1
Objectives	2
Approach.....	3
2 Hardware	5
EMI sensor	5
Cs vapor magnetometer.....	5
Fluxgate magnetometer	5
3 System Integration.....	7
Simultaneous operation of the GEM-3 and a Cs vapor magnetometer	7
<i>Background</i>	<i>7</i>
<i>Magnetometer placement</i>	<i>9</i>
<i>Compensation of EM-induced offsets</i>	<i>12</i>
Ergonomic development	16
<i>Sensor mounting hardware</i>	<i>17</i>
<i>Backpack</i>	<i>17</i>
<i>System weight and balance.....</i>	<i>17</i>
Power supply and electrical interface	18
Positioning system integration	19
Data handling	21
<i>Pre-processing.....</i>	<i>21</i>
<i>Processing.....</i>	<i>22</i>
4 Field Tests	23
Field Test 1: NRL Blossom Point UXO Test Site, MD	23
<i>Dynamic survey test description</i>	<i>23</i>
<i>Dynamic survey findings.....</i>	<i>24</i>
<i>Cued analysis tests</i>	<i>28</i>
Field Test 2: ERDC UXO Test Site, Vicksburg, MS	30
<i>Site description</i>	<i>30</i>
<i>Survey results.....</i>	<i>31</i>
Field Test 3: Aberdeen Proving Ground Standardized UXO Technology Demonstration Site, MD	33
5 Summary	35
References.....	36

Figures and Table

Figures

Figure 1. Man-portable dual EM73/magnetometer sensor.....	3
Figure 2. Cs magnetometer orientation requirements.	7
Figure 3. Observed, modeled, and residual EM-induced errors in measured magnetic data. EM73 transmit coil positions are shown in red. Asymmetry in residual error plot occurs near physical location of transmit driver interface connection.	9
Figure 4. Original magnetometer sensor location relative to peak EM field in GEM-3 cavity.	10
Figure 5. Nominal and worst case measured magnetic field errors as a function of the peak EM transmit field.	11
Figure 6. Revised magnetometer sensor location relative to peak EM field in GEM-3 cavity.....	12
Figure 7. Measured and modeled magnetic offsets induced by EM73 sensor.	13
Figure 8. Measured and predicted magnetic offsets induced by GEM-3 sensor. Predicted offsets assume an oscillating EM field only.	13
Figure 9. Magnetic offsets induced by GEM-3 as a function of frequency. For tests performed 6 July and 11 August 2004, the magnetometer was located in the center of the GEM-3 cavity.	14
Figure 10. Measured magnetic offsets induced by a constant EM field.	15
Figure 11. Measured and predicted magnetic offsets induced by GEM-3 operating at a single frequency (9.8 kHz). Predicted offsets are sum of AC and DC field effects.....	16
Figure 12. Measured and predicted magnetic offsets induced by GEM-3 transmitting multiple frequencies (3030, 6030, and 13050 Hz).	16
Figure 13. Dual-sensor system deployed in a hand-held configuration at Blossom Point UXO Test Site, MD.	24
Figure 14. Total magnetic field data collected at the Blossom Point UXO Test Site.	25
Figure 15. EM quadrature sum data collected at the Blossom Point UXO Test Site.	26
Figure 16. SNRs for dual-sensor data collected at the Blossom Point UXO test site.....	27
Figure 17. Comparison of GEM-3 and EM73 SNRs over selected targets at Blossom Point UXO Test Site.	27
Figure 18. Raw and filtered dual-sensor position data collected using the ArcSecond positioning system.	28
Figure 19. GEM-3 6030 Hz in-phase data collected using a template with static measurements (left panel) compared with data collected in a dynamic sweeping motion, positioned with the ArcSecond positioning system.	29
Figure 20. Quality of dipole-fit analysis as a function of sweep speed.	30
Figure 21. GEM-3 and magnetometry data collected with the dual-sensor system at the ERDC UXO Test Site.....	32
Figure 22. Dual-sensor SNR values for emplaced targets at ERDC UXO Test Site.	32
Figure 23. Dual-sensor system reconfigured into a push cart configuration.	33

Figure 24. An example of data collected at APG Standardized UXO Technology Demonstration Site. In-phase color EM data were converted to grayscale, and then transparent magnetometer data were overlayed onto grayscale EM data.	34
---	----

Table

Table 1. System weight summary for the GEM-3.	18
--	----

Preface

This report describes efforts undertaken as part of the Environmental Quality Technology (EQT) Program A (1.6.a), Unexploded Ordnance (UXO) Screening, Detection, and Discrimination Management Plan, UXO Detector Design Thrust Oversight (BA2/3) Major Thrust, UXO Technology Demonstration, Work Unit “UXO Hand-Held Sensor Design.” The work documented in this report was performed from 14 November 2003 through 31 May 2005. Dr. M. John Cullinane, Technical Director for Environmental Engineering and Cleanup, Environmental Laboratory (EL), U.S. Army Engineer Research and Development Center (ERDC), is the UXO Focus Area Manager for EQT. A BAA through Aberdeen Test Center funded the demonstration of the sensor at the Aberdeen Proving Ground Standardized UXO Technology Demonstration Site during the 30 May–7 July 2006 timeframe.

John Ballard, ERDC, and George Robitaille, U.S. Army Environmental Center (USAEC), were program managers of the EQT Program A (1.6.a) UXO Screening, Detection, and Discrimination Management Plan during the execution of this project. Principal investigators for this work were Hollis “Jay” Bennett, EL, ERDC, and David Wright, AETC Inc.

This project was performed under the general supervision of Dr. David Tazik, Chief, Ecosystems Evaluation and Engineering Division, and Dr. Elizabeth C. Fleming, Director, EL.

COL Richard B. Jenkins was Commander and Executive Director of ERDC. Dr. James R. Houston was Director.

1 Introduction

This report documents the activities of the project “Improvements to the Hand-held Dual Magnetic/EMI Sensor.” It was conducted 14 November 2003 to 31 May 2005. Aberdeen Test Center funded a separate demonstration of the sensor at the Aberdeen Proving Ground (APG) Standardized Unexploded Ordnance (UXO) Technology Demonstration Site during the 30 May to 7 July 2006 timeframe. The demonstration is discussed in Chapter 4 of this report, under “Field Test 3: Aberdeen Proving Ground Standardized UXO Technology Demonstration Site, MD.”

During the 14 November 2003 to 31 May 2005 period, AETC Incorporated improved on the EM73/magnetometer dual sensor that was developed under a previous project entitled “Hand-Held Dual Magnetic/EMI Sensor.” This original instrument successfully combined both electromagnetic (EM) and magnetic sensor technology; however, it was limited both ergonomically and by the fact that it operated at a single EM frequency. In the current project these limitations were overcome by combining a light-weight, multi-frequency EM sensor (the GEM-3 developed and produced by Geophex Ltd., Raleigh, NC) with a commercial off-the-shelf Cesium (Cs) vapor magnetometer (model 823A produced by Geometrics, Inc., San Jose, CA). This report describes the technical issues addressed during the development of this instrument and presents the results of two field trials performed with this instrument.

Background

Electromagnetic induction (EMI) and total magnetic field surveys are the two primary geophysical technologies used for UXO detection. Hand-held EMI sensors perform better against shallow UXO items, and can detect nonferrous sub-munitions. Cesium vapor magnetometers are effective against large, deep ordnance items that hand-held EMI sensors cannot detect; however, they do not respond to nonferrous objects. On sites requiring the use of both technologies, the cost of collecting these data sets is significantly reduced if the data are collected simultaneously in a single survey. In addition, simultaneous data acquisition provides accurate relative positioning of the two data sets. This accuracy, particularly in the vertical dimension, is a prerequisite for the successful application of advanced joint/cooperative inversion algorithms currently under development.

The technical barrier to simultaneous collection of EMI and total magnetic field data lies in the deleterious effect of the EMI transmitted field on the magnetic field measured by the Cs vapor magnetometers. These magnetometers track oscillations of the magnetic field occurring at frequencies <200 hertz (Hz). For magnetic field oscillations $\gg 200$ Hz they simply measure the average effect of these oscillations. Thus, the large low frequency components of a time domain EM field distort the measured geomagnetic field, but a constant wave frequency domain EM (FDEM) sensor operating well above 200 Hz only induces an offset in the measured magnetic data. The magnitude of this offset is a function of the strength and orientation of the transmitted EMI field relative to the Earth's geomagnetic field vector.

In a recent project sponsored by the U.S. Army Engineer Research and Development Center (ERDC), the viability of combining an EM sensor with a Cs vapor magnetometer was demonstrated. During this project, it was shown that the effect of an EM field on the measured magnetic field can be predicted. This effect can be mitigated in a number of ways. Maximizing the physical separation of the sensors reduces the magnitude of the EM field (thus its effect), but the ability to do this with a hand-held sensor is limited. If the orientation of the instrument relative to the Earth's magnetic field is held constant (as during cued target investigations), the EM effect on the measured total magnetic field would be a simple offset. Similarly if this orientation varies with a periodicity that is much greater than that of the target response, the resulting effect can be removed with appropriate spatial or temporal filters similar to those used to remove background and geologic signal. Finally, in areas where topography or vegetation cause large and abrupt orientation changes, a fluxgate sensor monitors orientation changes (relative to the Earth's field), allowing prediction and removal of the EM effect from the measured magnetic response.

Objectives

The objective of the project was to implement and test modifications to the ERDC EM73/Magnetometer sensor technology that was configured by AETC on behalf of the ERDC under contract DACA42-02-C-0049. These modifications were intended to improve the utility of this sensor with respect to its mode of deployment and its detection/classification capability. In its current configuration, the dual EM73/magnetometer sensor is deployable only due to ergonomic reasons in the man-portable, wheel-mounted mode shown in Figure 1. Operation of the sensor in a true

hand-held configuration would require compensation of magnetometer heading errors induced by proximity to the EM sensor as well as ergonomic improvements consisting primarily of weight and balance improvements. An additional objective of this project was to improve the detection and classification performance of this technology through the addition of multi-frequency EM capability. The task of integrating the instrument with an ArcSecond positioning system was added to provide improved sensor positioning.



Figure 1. Man-portable dual EM73/magnetometer sensor.

Approach

Tests performed with an early version of the Geophex model GEM-3 frequency domain sensor showed that it did not transmit a continuous wave EM signal and was therefore discounted as a suitable instrument for simultaneous deployment with a magnetometer sensor. At the suggestion of Dr I.J. Won (Geophex Ltd), an upgraded version of the GEM-3 was tested. This “enhanced” version was found to transmit a continuous wave signal. Incorporation of this sensor into a dual-sensor instrument provides the advantages of significant weight reduction and multi-frequency capability. Modifications to the GEM-3 console provided the capability of logging positioning data (using National Marine Electronics Association (NMEA) standard data formats common to most global positioning system [GPS] receivers) as well as an additional serial data string. For the application at hand, this data string was comprised of the magnetic data output from a Geometrics model 823A Cs vapor magnetometer. This

particular magnetometer came with an internal counter (to convert the Larmor signal to magnetometer values) as well as a 5-channel analog to digital (A/D) converter. This A/D capability was used to convert analog voltages from a Barrington model MAG-03-MN three component fluxgate magnetometer into digital format, and transmitted as a single serial data string to log the Cs and fluxgate magnetometer data.

After procurement of the EMI sensor and a Cs vapor magnetometer, a series of static tests were performed. These tests were designed to characterize the EMI sensor effect on the measured magnetic data and define the conditions by which the two technologies could be coupled for simultaneous deployment.

Subsequent to the static tests and partially based upon the findings of these tests, the magnetometer was physically integrated with the EMI sensor, and two separate field trials were performed. The first field trial was performed at the Naval Research Laboratory (NRL) Blossom Point test facility near La Plata, MD and was used primarily as a system “shakedown” test to verify sensor operation in both dynamic and cued investigation modes. Operational procedures for both modes were tested and finalized during this trial. A second field trial was performed at the ERDC UXO test site in Vicksburg, MS. The goal of this trial was to demonstrate and verify sensor operation in a benign topographic and geologic environment.

2 Hardware

The system hardware comprises an EMI sensor, Cs vapor magnetometer, fluxgate magnetometer, hand-held data acquisition computer, integrated power supply, interconnection cables, and deployment hardware (e.g., backpack and mounting pole).

EMI sensor

The EMI sensor selected for this project was a conventional GEM-3 developed and manufactured by Geophex Ltd. This sensor was a relatively recent version commonly referred to as the 'enhanced GEM-3' to differentiate it from older vintages. The GEM-3 is a frequency domain sensor capable of operation at multiple, user selectable frequencies between 30 Hz and 24 kilohertz (kHz). The GEM-3 can be used with 40-, 64-, or 96-centimeter (cm) diameter coil heads. The 64-cm head was selected for this project to maximize the depth of investigation as well as provide sufficient area around the coils for mounting of the Cs sensor. The 96-cm head would have also accomplished these objectives, but it is not suitable for hand-held deployment.

Cs vapor magnetometer

The magnetometer selected for this project was a Geometrics model G823A. This sensor has the Larmor signal de-coupler and counter mounted in the preamp electronics package. This configuration negates the requirement for an additional console, thus reducing the complexity of the survey deployment mechanics. This sensor provides total magnetic field readings (units are nano-Tesla [nT]) at a 10-Hz sample rate in ASCII* format via a serial RS232 data connection.

Fluxgate magnetometer

A Bartington model Mag-3MRN60 3-axis fluxgate magnetometer (Bartington Instruments, Oxford, England) was selected to provide the instrument attitude relative to the Earth's magnetic field. This sensor converts the three components of the Earth's field into voltages at a sensitivity of 24 nT/millivolts (mv) (- 60,000 to + 60,000 nT is equivalent to a full scale of 0 to 5000 mv). Based upon this sensors specifications and

* ASCII - American Standard Code for Information Interchange.

calibration data, it provides a measure of the angle of the Mag/EM instrument relative to the Earth's field with an accuracy of less than 1 degree.

3 System Integration

During this project, the tasks involved in integrating the various sensors into a UXO survey instrument included:

1. Defining the conditions required for operation of the magnetometer in the presence of an EM field;
2. Ergonomic development providing sensor mounting hardware for hand-held deployment;
3. Electrical integration of the various sensors including development of appropriate power supply and electrical interfaces; and
4. Integration of a suitable positioning system.

Simultaneous operation of the GEM-3 and a Cs vapor magnetometer

Background

A Cs vapor magnetometer provides a measure of the magnitude of the Earth's magnetic field vector. The limitations of this measurement are that the magnitude is between 20,000 and 100,000 nT and that this vector intersects the longitudinal axis of the magnetometer at 45° plus or minus 30° as depicted in Figure 2.

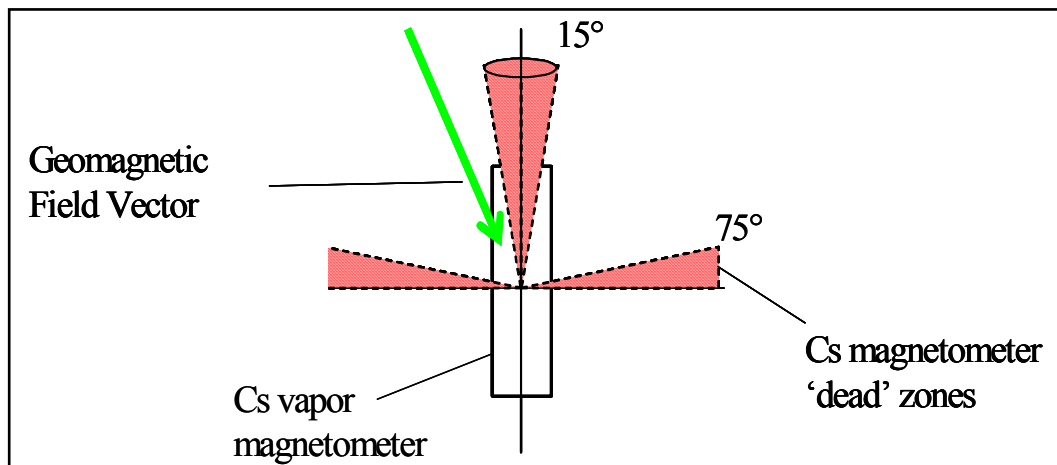


Figure 2. Cs magnetometer orientation requirements.

The EM sensor causes the Earth's magnetic field to oscillate at the EM transmit frequency. The magnetometer measures the magnitude of the Earth's magnetic field vector. This vector is the vector sum of the Earth's static field and the oscillating EM field. For fields oscillating at much

greater than 200 Hz, the magnetometer measures the average effect of these fields (confirmed by Kenneth Smith of Geometrics Ltd). The average effect of that component of an EM field that is aligned with the Earth's magnetic field will be zero; however, the component of the EM field that is normal to the Earth's field will always result in an increase in the magnitude of the measured total field. The magnitude of the Earth's field vector in the presence of an oscillating EM field can be expressed as:

$$H_{meas}^2 = \langle H_{earth}^2 + H_{orth_EM}^2 \rangle \quad (1)$$

Where $\langle \rangle$ denotes time averaging, and H_{orth_EM} represents the component of the time-varying EM field that is orthogonal to the Earth's field vector.

Under the assumption $H_{earth} \gg H_{orth_EM}$, the resulting effect of the EM field (i.e., the EM-induced heading error) can be expressed as:

$$H_{err} = \frac{1}{2} \langle H_{orth_EM}^2 \rangle \div H_{earth} \quad (2)$$

The left panel of Figure 3 shows the observed heading errors over a horizontal plane 0.25 m above the EM73 sensor operating at 9.8 kHz. With the magnetometer sensor positioned at each grid node, the EM sensor was cycled on and off and the resulting offsets are the induced heading errors. These observed errors are juxtaposed with the modeled EM-induced heading errors in the center panel and the residual errors (after subtracting the modeled errors from the observed errors) on the right. The modeled data were based on a coarse estimate of the total magnetic field vector components (derived from the geographic position of the sensor and the International Reference Geomagnetic Field model 2000 (IGRF2000)). These results indicate that, given a measure of the combined sensor attitude with respect to the Earth's magnetic field, it is possible to compensate for EM-induced heading errors.

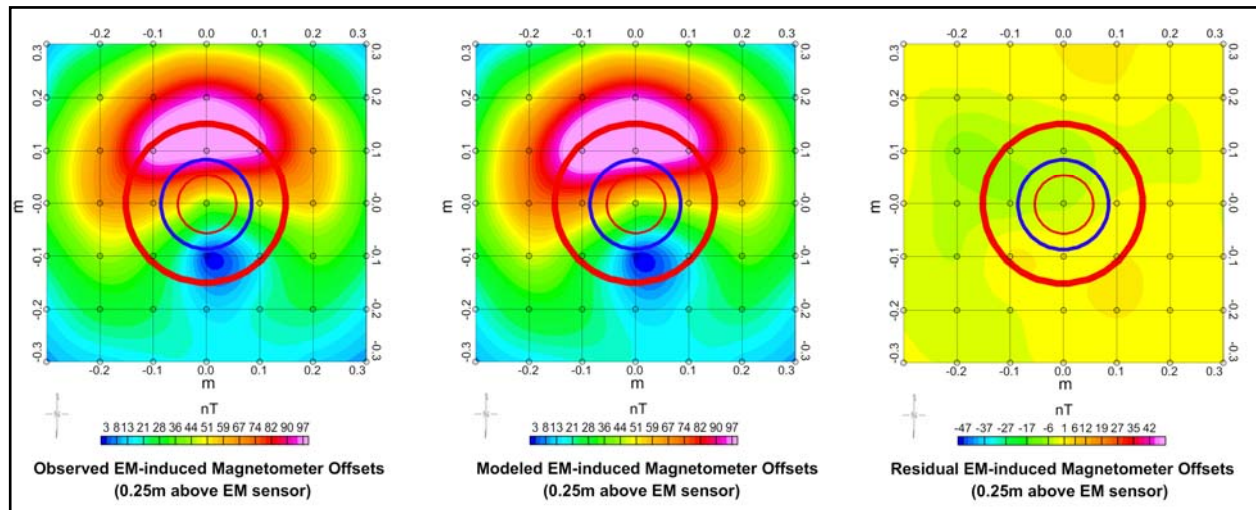


Figure 3. Observed, modeled, and residual EM-induced errors in measured magnetic data. EM73 transmit coil positions are shown in red. Asymmetry in residual error plot occurs near physical location of transmit driver interface connection.

Additional consideration needs to be paid to the effect of the instantaneous EM field. A continued increase in this field will eventually cause the net magnetic vector to violate the operating limits of a Cs vapor magnetometer by exceeding the dynamic range of the magnetometer or by causing the intersection angle of the vector to fall too close to the magnetometer's longitudinal or lateral axis. In a hand-held deployment device, the orientation of the magnetometer with respect to the Earth's field is variable and must be constrained to ensure that the intersection angle limits are not violated (Campbell 1997). It follows that distortion of the Earth's vector angle by an EM field will impose additional constraints on the magnetometer orientation. For this reason, minimization of the magnitude of the EM field at the magnetometer was an important consideration for this project.

Magnetometer placement

Ergonomic considerations dictated that the magnetometer be mounted within the coil assembly cavity. Figure 4 shows the net EM transmit field (peak) and the initial placement of the magnetometer sensor. This image shows a vertical cross-section of the field within the coil cavity. The innermost coil is the receive coil (cross section shown in blue). This coil defines the physical limits of the coil assembly cavity. The magnetometer senses the net magnetic field vector over a 1 in. high by 1 in. diameter cylindrical volume. Figure 4 shows this cylinder positioned at the center of the EM coil assembly.

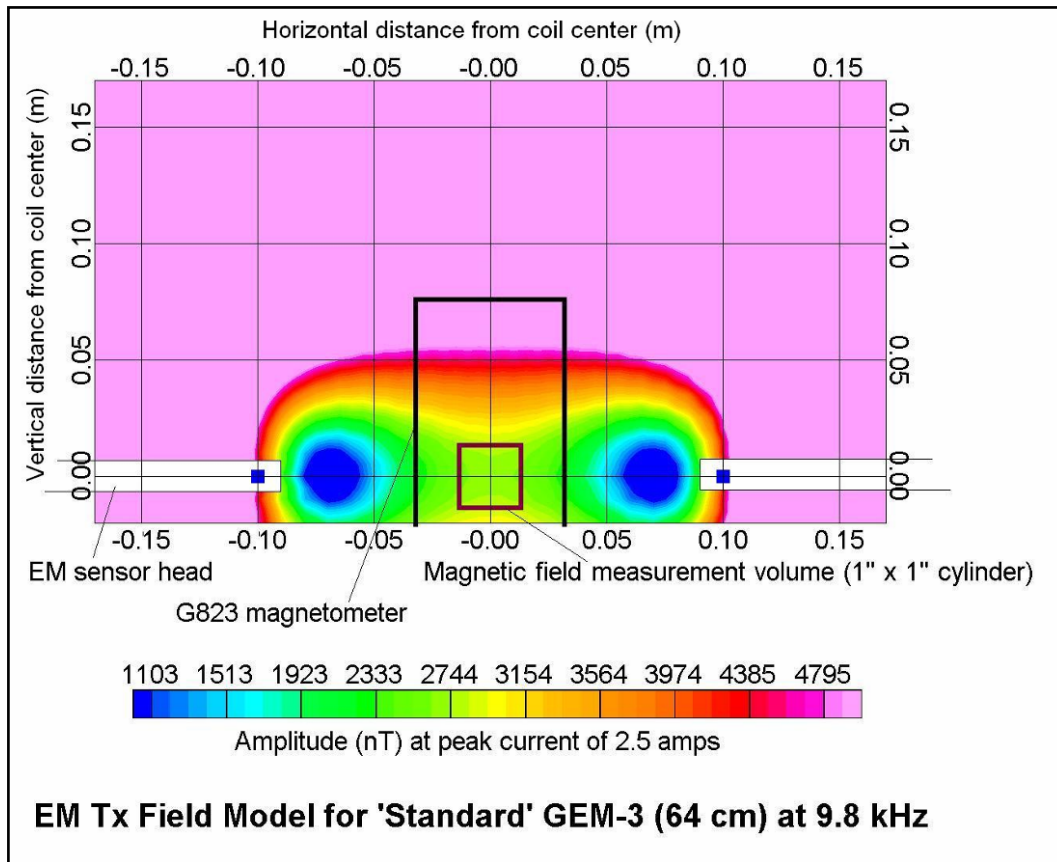


Figure 4. Original magnetometer sensor location relative to peak EM field in GEM-3 cavity.

The EM-induced error is a function of the magnitude of the EM field and its orientation relative to the Earth's field. Figure 5 shows the EM-induced offset as a function of an EM field magnitude for two orientations. The blue curve shows the expected offset for a level sensor (the inclination of the Earth's field is assumed to be 65°) and the red curve shows the worst-case offset where the EM field is normal to the Earth's field. Figure 5 shows that the GEM-3, operating at 9.8 kHz with a peak current of 2.5 amps produces an EM field magnitude of approximately 2,750 nT (indicated by the green arrow). The GEM-3 will output up to 10 amperes of current depending on the transmit frequency (lower frequencies result in higher transmit currents). Higher current produces much higher EM induced errors and also results in tighter operational restrictions on the orientation of the instrument during a dynamic survey.

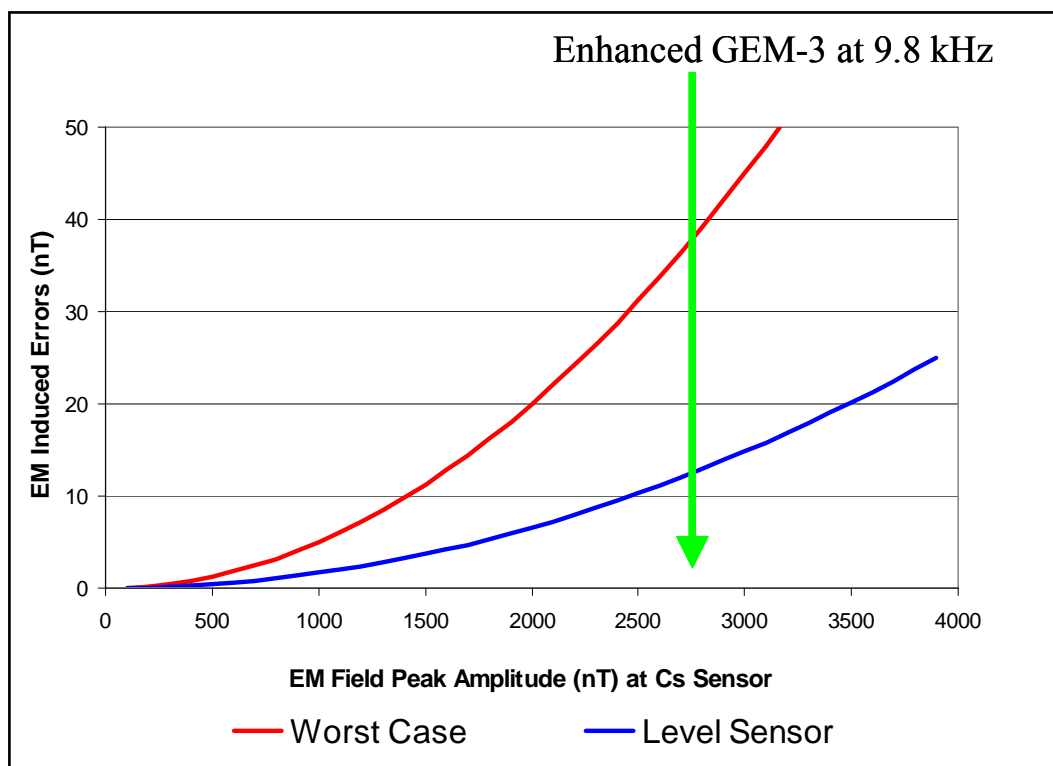


Figure 5. Nominal and worst case measured magnetic field errors as a function of the peak EM transmit field.

With a minor modification to the GEM-3 coil assembly, the magnetometer was positioned in a region within the coil cavity where the EM field over the sensing volume of the magnetometer would be greatly reduced. This modification involved removing some of the support material along part of the physical cavity to allow the sensor to be placed directly beside the EM receive coil, as shown in Figure 6. This design modification reduced the effective EM field amplitude by an approximate factor of 4.

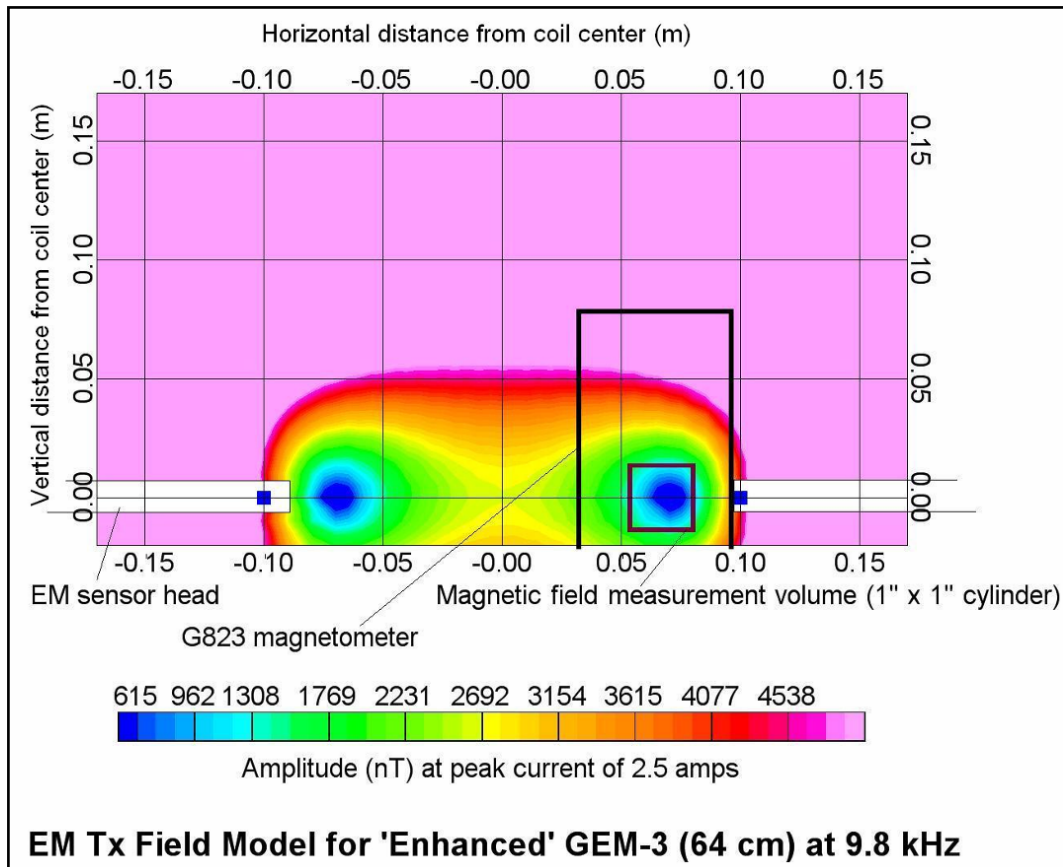


Figure 6. Revised magnetometer sensor location relative to peak EM field in GEM-3 cavity.

Compensation of EM-induced offsets

For deployment under dynamic conditions where the orientation of the instrument is highly variable, the expected magnitude of the induced offset can be calculated if the angle of intersection of the EM field with the Earth's field (at the magnetometer) is known. Figure 7 shows both the observed and calculated offsets induced by an EM73 sensor as a function of this angle. The magnetometer was rigidly connected to the EM73 with the sensing volume of the magnetometer on the same plane as the EM coils and offset from the center of these coils by 30 cm. Logically, as the intersection angle (θ) approaches zero, so too does the magnitude of the observed offset. When the same test was performed with the GEM-3 (operating at the same frequency), however, this was not the case. Figure 8 shows that the observed data appear to approach a non-zero value as θ approaches zero. Furthermore, at some frequencies (e.g., 12,030 Hz) this value can be negative. The only plausible explanation for this effect is that a direct current (DC) field is also being transmitted by the GEM-3 (because all alternating current [AC] fields must impose a positive bias).

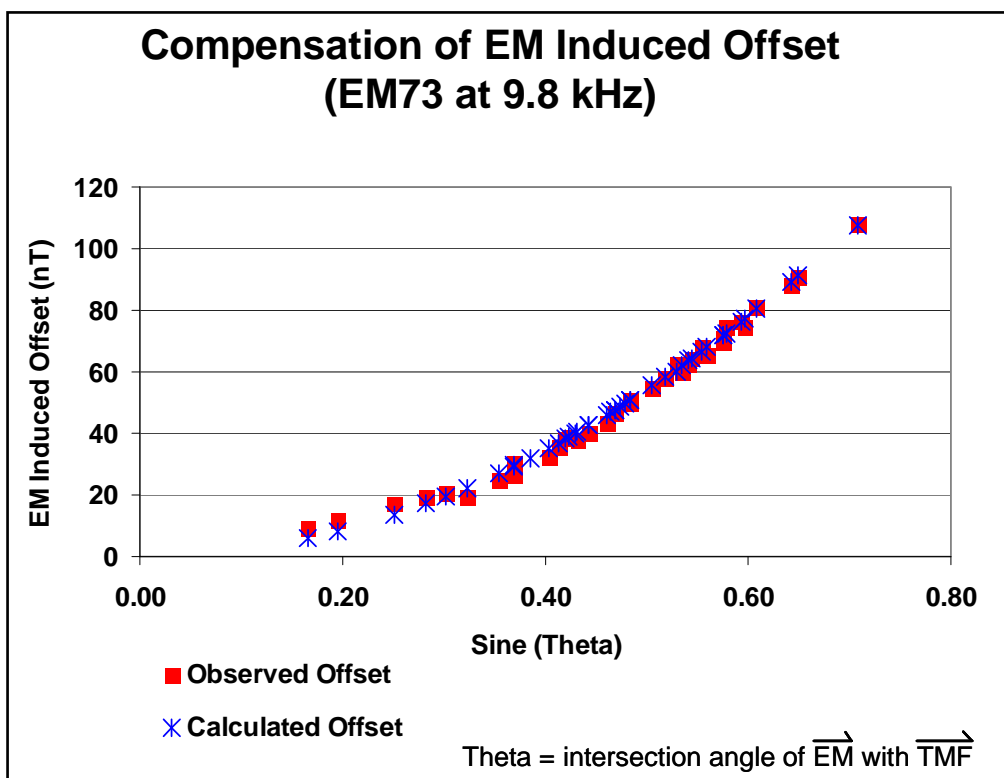


Figure 7. Measured and modeled magnetic offsets induced by EM73 sensor.

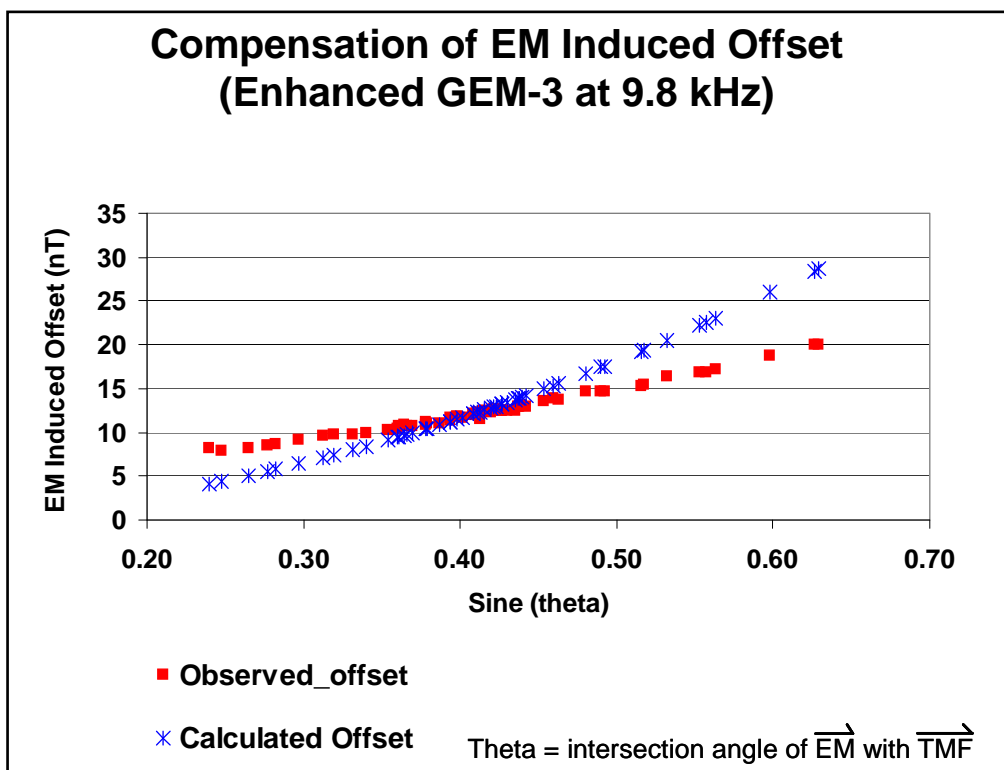


Figure 8. Measured and predicted magnetic offsets induced by GEM-3 sensor. Predicted offsets assume an oscillating EM field only.

Unlike the EM73 results, the GEM-3 induced offsets do not approach zero as sine (theta) approaches zero. One postulation is that this phenomenon is due to residual DC currents flowing in the GEM-3 transmitter (TX) coils. These currents are very small and are believed to be a result of the digital synthesized wave form that the GEM-3 employs. Further evidence of this effect is that this DC current-induced offset varies with frequency. Figure 9 shows the EM-induced offset as a function of frequency (using a single GEM-3 frequency) for three separate tests. The first two tests were performed with the magnetometer located in the physical center of the EM coils, and the last test was performed with the magnetometer in its final location. Those frequencies where the offset is significantly smaller than their adjoining frequencies will result in a negative offset when sine (theta) is zero. This negative offset also indicates that there must be some DC current-induced offset because AC fields cannot cause a negative offset.

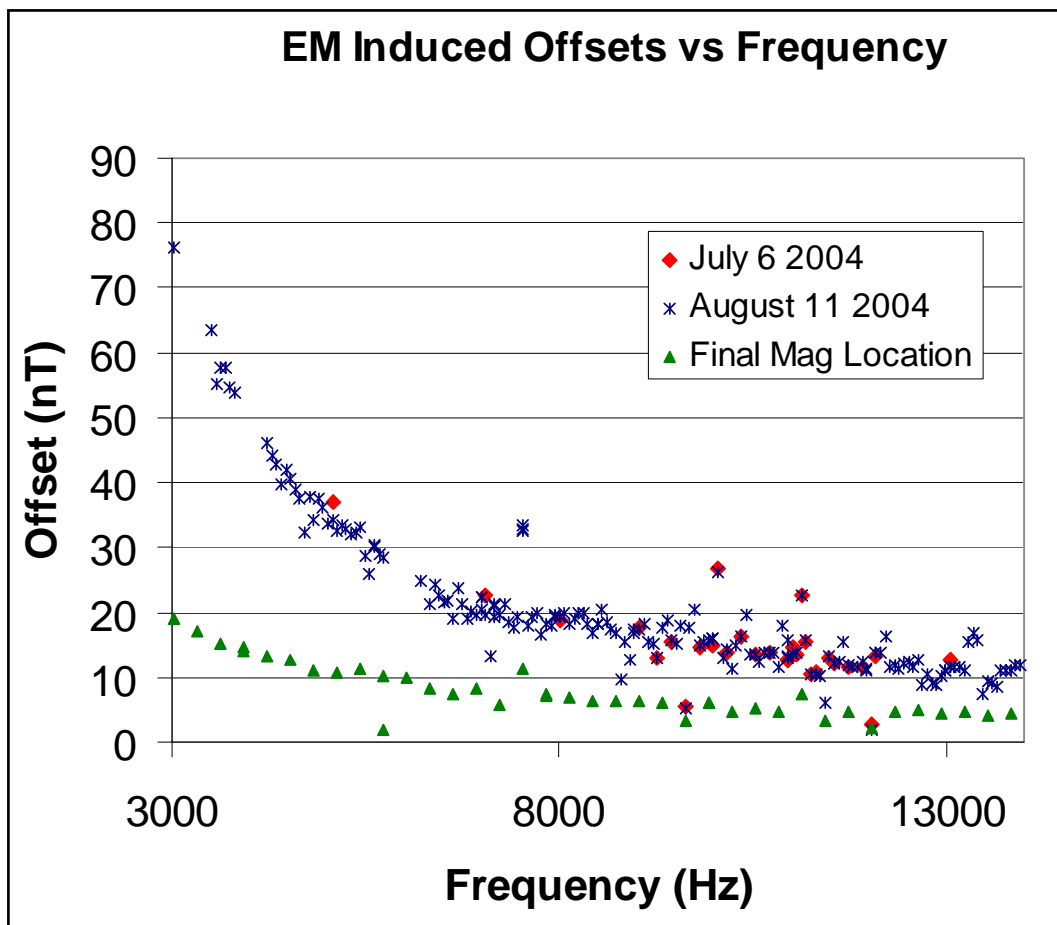


Figure 9. Magnetic offsets induced by GEM-3 as a function of frequency. For tests performed 6 July and 11 August 2004, the magnetometer was located in the center of the GEM-3 cavity.

The mechanism by which a DC field affects the magnetic field is similar to that of an AC field, with some important differences. The component of the DC field that is aligned with the Earth's magnetic field will either directly add to or subtract from the Earth's field. For an AC field, this component averages to zero. The residual DC field transmitted by the GEM-3 is very small relative to that of the AC field. Because the DC field is so weak, the component of the DC field that is normal to the Earth's field has a negligible effect on the total magnetic field. The result is that the DC field can impose a negative or positive offset on the measured total magnetic field (Figure 10), and this offset is maximized when the DC field is aligned with the Earth's field (i.e., this effect is orthogonal to that of an AC field).

Thus, for applications where the effect of the GEM-3 transmit field must be compensated for, the compensation must include a correction for both the AC field effects and the DC field effects. Figure 11 illustrates the results of this compensation for a single frequency (9.8 kHz) with the magnetometer located in the center of the GEM-3 coil assembly. Figure 12 shows the same results for multi-frequency operation of the GEM-3 with the magnetometer located in the final "offset" position.

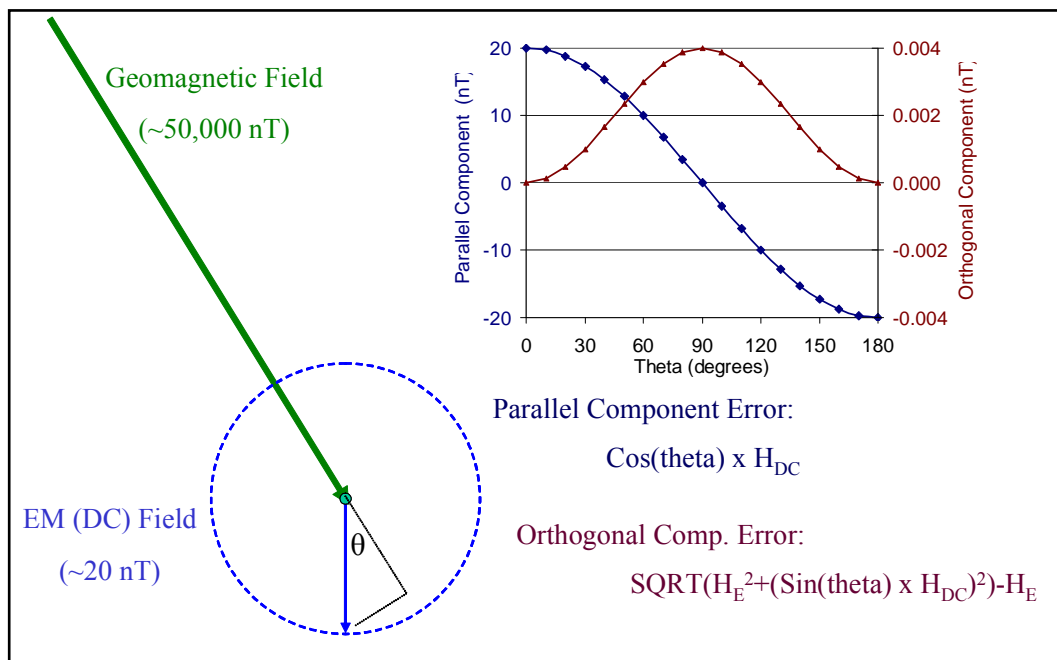


Figure 10. Measured magnetic offsets induced by a constant EM field.

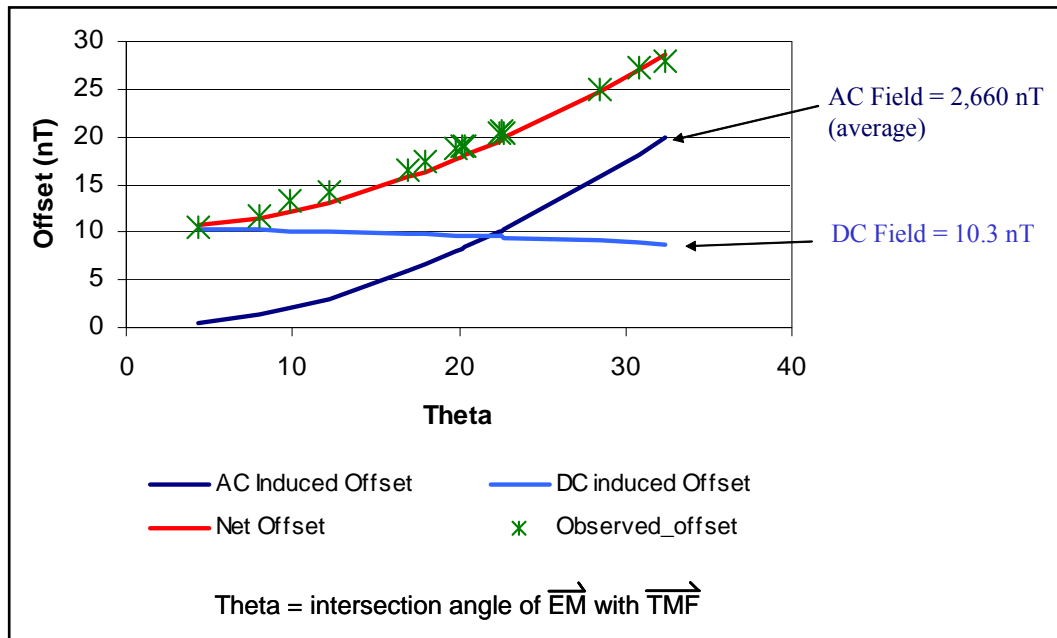


Figure 11. Measured and predicted magnetic offsets induced by GEM-3 operating at a single frequency (9.8 kHz). Predicted offsets are sum of AC and DC field effects.

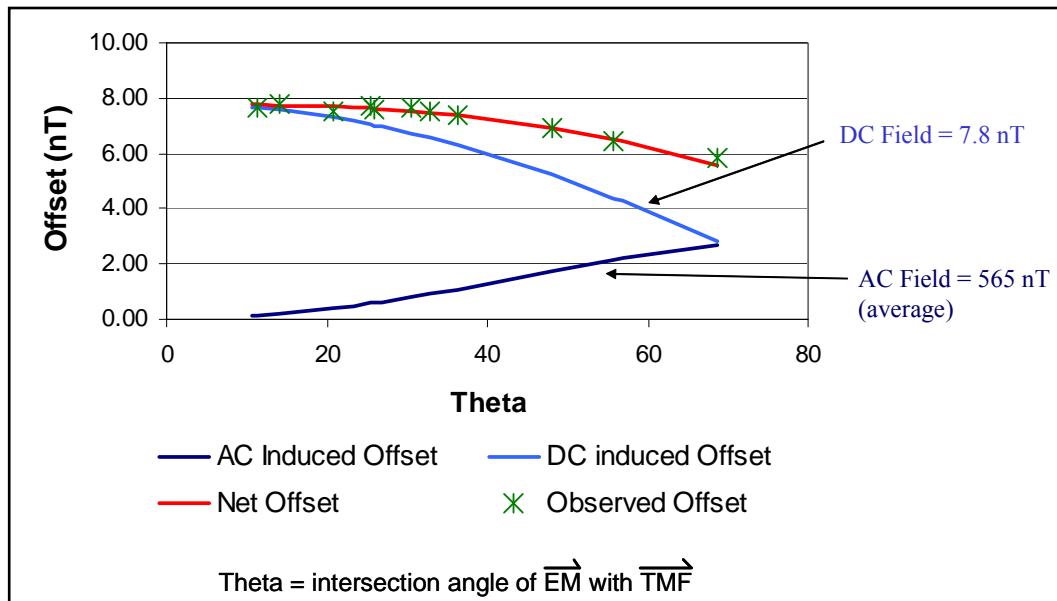


Figure 12. Measured and predicted magnetic offsets induced by GEM-3 transmitting multiple frequencies (3030, 6030, and 13050 Hz).

Ergonomic development

One of the goals of this project was to provide a hand-held version of the dual-sensor technology. This required modifications to the GEM-3 deployment hardware and the addition of a suitable backpack to carry the batteries, magnetometer preamp/counter assembly, and positioning system hardware. Hand-held deployment also required that the overall

system weight be minimized and that the weight carried on the sensor mounting pole be balanced appropriately.

Sensor mounting hardware

The original hardware used for deployment of the GEM-3 consisted of a lightweight, expandable carrying pole. The GEM-3 console was mounted at the top of the pole and the iPAQ™ data logger was mounted midway along the pole. The GEM-3 coil assembly was attached at the bottom of the pole. Adding the magnetometer sensor required that it be positioned in close proximity to the EM coils and that its positioning relative to these coils was fixed. The weight to the sensors on the bottom end of the carrying pole caused an undesirable flexing and bouncing. The original pole and coil mounting assembly were replaced with more rigid components. A suitable mounting bracket was designed and manufactured by Raleigh Plastic, Inc., Raleigh, NC, and the flexible pole was replaced with a 1-in.-diameter fiberglass rod. In response to the added requirement of integration with a positioning system, an antenna mount was added to the top end of the pole. Finally a couple of control “arms” were added to the pole to provide a means to manually stabilize the sensor attitude.

Backpack

The addition of the magnetometers (Cs vapor and fluxgate) resulted in the need to carry an additional power supply as well as the Cs vapor magnetometer preamp/counter assembly. A lightweight, all plastic frame backpack was selected to carry all ancillary instrumentation. The frame also provides an attachment point for the straps used to support the weight of the carrying pole.

System weight and balance

For a hand-held sensor, weight minimization and distribution are important concerns. The GEM-3 as shipped weighs approximately 9 lb. However, the addition of the Cs and fluxgate magnetometers, cabling, power supply, and sensor mounts brings the total system weight to 27.5 lb, excluding the weight of a positioning system. Traditional GPS systems will weigh less than 5 lb; however, the ArcSecond positioning system specified by the ERDC for this development adds 18.5 lb to the total system weight (for a total of 46 lb). Table 1 shows the total system weight for different positioning schemes.

Table 1. System weight summary for the GEM-3.

	Positioning System		
	None	GPS	ArcSecond
Backpack	11.00	14.00	25.50
Carry Pole	16.50	18.50	20.50
Total (lb)	27.50	32.50	46.00

The weight of the carry pole is supported by two straps that are attached to the backpack, thus the entire load is distributed to the shoulders and hips by the backpack. The system is currently configured so that the center of gravity falls directly under the attachment point on the backpack when the ArcSecond antenna triad is attached. For other configurations, the straps and pick-up points are easily configured to maintain the same balance.

Power supply and electrical interface

The GEM-3 comes equipped with an internal 12 volts DC (VDC) power supply that will run the GEM-3 for up to 5 hours. Unfortunately this battery is not easily replaced and requires charging between combined sorties that will exceed 5 hours. The Cs and fluxgate magnetometers both require 24–28 VDC power. To provide this power, a pair of 11.5 VDC, lithium-ion batteries is used to provide voltage via a Vicor™ power converter. This arrangement will power the magnetometers for up to 10 hours. In addition, the batteries are easily replaceable between sorties.

Analog signals from the Bartington fluxgate are directed to the analog to digital (A to D) converter in the G823A electronics package. These data are appended to the Cs magnetometer output and transmitted via RS232 data link to the GEM-3 console. In a similar fashion, the positioning data are transmitted from the positioning system to the GEM-3 console. The GEM-3 console time stamps the magnetometer data and the EM data and transmits these data and the position data to the iPAQ™ data logging device. The position data arrive at the GEM-3 console with a time stamp. When a GPS (or in the case of the ArcSecond system, a GPS look-alike system) is used, the GEM-3 console time is synchronized to that of the positioning system to ensure proper time alignment of the various sensor inputs (discussed in greater detail in the next section).

Positioning system integration

AETC Inc. was tasked with the design requirement of integrating the dual-sensor with a positioning system that ArcSecond Inc. was adapting for UXO applications. The ArcSecond system configured for this application comprised two or more remote beacons and an array of three sensors that were mounted on the structure that was being positioned. In this case the structure was the dual-sensor carry assembly. The beacons transmitted a timing pulse and two rotating lasers. Upon detection of these lasers, each sensor provided a measurement of the vertical and horizontal angle of the sensor position relative to the transmitting beacon. Having accurate measures of each beacon's position and orientation, these angles were used to triangulate the sensor positions in three dimensions. As the positions of each of the three positioning sensors in the array were measured, the position and orientation of the geophysical sensors (assuming that the positioning sensor array is fixed rigidly to the geophysical sensor carry assembly) were calculated.

Because the ArcSecond system uses angular measurements from the beacons rather than distance measurements, the setup and calibration of the beacon positions is more complex than that for other systems. The position and orientation of each beacon must be precisely measured and very stable. Each deployment must be followed by a calibration of the system where six or more measurements are taken so that the beacon locations and orientations can be determined relative to each other. The sensors are then positioned during the course of the geophysical survey relative to the beacon network frame of reference. These positions can then be translated to a local or standard coordinate system.

An important consideration for integration of the positioning system with geophysical sensors is that of time alignment. For dynamic applications, it is necessary to align the time of applicability (TOA) of the geophysical sensor data with the time of applicability of the measured positioning data to within 1 millisecond. Any measurement will have some latency before the data are collected and stored. This latency may be static in nature or it may have some variability. In addition to this latency, conventional time stamping of RS232 data is not precise and can inject 100's of milliseconds of additional delays. Thus, simply time stamping the positioning data as it is transmitted to the GEM-3 console does not ensure that the TOA of the positions can be precisely aligned with that of the geophysical data.

In the integration of the ArcSecond positioning system with the dual-sensor, this problem is addressed by using a time alignment scheme similar to that used when GPS systems are integrated with geophysical sensors. The ArcSecond system was modified to emulate GPS systems by providing a pulse per second (PPS) trigger pulse and standard NMEA data strings via an RS232 data link. This provides for interoperability of the ArcSecond system with any geophysical systems that are currently capable of integration with GPS systems.

GPS systems commonly have an internal latency that is variable (i.e., the time between the applicability of a given measurement and the transmission of the derived position will vary) in addition to the serial port variability. To allow users to know precisely when a measurement applies to any given position, the data message is time stamped (i.e., the position solution is given in four dimensions; time, x, y, and z) to a very high degree of precision. In addition GPS receivers will also output a PPS trigger at every precise integer second as a means to synchronize associated data acquisition with GPS time. The integer ambiguity of the PPS trigger is resolved by sending the data acquisition system a message (via RS232) that is used simply to assign the precise time to the incoming PPS trigger.

To ensure compatibility with the GEM-3 firmware, the transmitted data consists of two standard NMEA messages \$GPZDA and \$GPGGA. The \$GPZDA message allows the GEM console to assign the correct integer time to the next PPS signal. This is the primary basis of time alignment between the two systems. The GEM-3 console uses the PPS and the \$GPZDA message to discipline its internal clock to be the same as that of the ArcSecond system. Thus the time stamp applied to the geophysical data will be in the same timeframe as that being applied to the positioning data. This allows for the precise alignment of the geophysical data with the positioning data during post-processing. The \$GPGGA data contains real-time positions of one of the triad position sensors (complete with time of applicability). The actual positions of the geophysical sensors are calculated using ArcSecond post-processing software based upon the position and orientation of the ArcSecond position sensor triad.

It bears note that these NMEA formats were used out of expedience. The time and position data need not be related to any outside frames of reference (i.e., the time does not have to be accurate with respect to Coordinated Universal Time), but it must reflect the ArcSecond system time precisely. Similarly the positions are not necessarily accurate WGS84

mapped positions, but they must be precise relative to each other. The time and position data are output in the appropriate fields. Other fields may be used for other relevant data but are not required to contain the data described by the NMEA definitions.

It is possible for the data rates of the ArcSecond system to exceed the capacity of the GEM-3 interface. In its current configuration, the ArcSecond system can provide the position for one of the triad sensors in real time and be merged with the geophysical data based upon a precise (relative to the ArcSecond time base) time stamp.

Data handling

The process of transforming raw data collected during a geophysical survey into spatially registered geophysical data suitable for analysis may be logically divided into pre-processing and processing stages. The pre-processing stage involves transcribing the instrumentation-specific raw data files into a database format where the geophysical sensor data, ancillary data (e.g., three-axis fluxgate data), and position data channels are aligned with respect to their time of applicability. The processing stage involves application of filters and/or corrections to the various data channels to reduce noise in the geophysical signal. In a UXO survey this involves reducing sensor noise, geologic response, and baseline drift. Spatial co-registration of the final geophysical sensor data is also performed during this stage.

Pre-processing

The raw data samples from the GEM-3 and magnetometer (remembering that the magnetometer data sample record also contains the fluxgate data) are time-stamped by the GEM-3 console and transmitted to the iPAQ™ data logger where they are saved in a binary data file. When the ArcSecond positioning system is used with this system, a pseudo pulse per second and corresponding time message are used to discipline the GEM-3 console time to that of the ArcSecond system. The ArcSecond position data are stored and processed separately to provide a file containing a time-stamped position of the center of the GEM-3 coil assembly.

The steps used to transcribe these raw data files into two separate Geosoft databases (one for the magnetometer data and one for the GEM-3 data) are as follows:

1. Run [GEMExport.exe](#) to convert Geophex binary raw data to ASCII 'csv' files. The binary data file *{filename}GEM.gbf* will be split into a file for the GEM-3 data called *{filename}GEM.csv* and a separate file for the mag data called *{filename}GEM_AUX.csv*
2. Import the *{filename}GEM.csv* file into a geosoft database using the [GEM.i3](#) template
3. Import the *{filename}GEM_AUX.csv* file into a separate geosoft database (use the [GEM_AUX.i3](#) template)
4. Edit the raw position data provided by ArcSecond to:
 - a. if necessary, combine subsets of data into one data file for each sortie
 - b. search and replace all semicolons with commas.
5. Use the macro in the [reformat_macros_v2.xls](#) to convert the edited position data file into a TBL file. Note that the time base used (dtb_time) is in milliseconds
6. Merge the position data in the TBL file into each of the mag and EM databases.

Processing

The processing steps required to remove unwanted signal from the geophysical data were generally site-specific, but there were general procedures that performed this task.

Low pass filters were applied to remove very high frequency responses from the geophysical data that are normally due to sensor noise and/or platform vibration. These filters can also be applied to the positioning data to remove variations that are of too high magnitude to be realistic.

Demedian filters or similar processes that remove long wavelength features were useful for removing geologic response, sensor drift (EM), and diurnal variations (mag).

The dual EM/mag sensor also required removal of the EM-induced magnetic signal from the magnetometer data. For most surveys this signal was removed as part of the removal of long wavelength features. However, surveys conducted in areas where the sensor orientation relative to the Earth's field was rapidly changing (usually due to rugged terrain), required that the magnetometer data be corrected (see section "Compensation of EM-Induced Offsets."

4 Field Tests

The final phase of this development project involved performing two shakedown trials and one demonstration of the dual-sensor system. The first shakedown was performed at the NRL Blossom Point UXO Test Site. The objective of this trial was to test and finalize the sensor deployment procedures in both a dynamic survey mode for ordnance detection and a cued analysis mode for ordnance discrimination.

The second trial was performed at the ERDC UXO Test Site in Vicksburg, MS. The goal of this trial was to demonstrate and verify sensor operation in a benign topographic and geologic environment.

The third deployment was a system demonstration performed at the APG Standardized UXO Technology Demonstration Site, MD.

Field Test 1: NRL Blossom Point UXO Test Site, MD

Dynamic survey test description

This trial was fielded 21–25 February 2005. A dynamic survey for UXO detection was performed over the NRL Blossom Point UXO Test Site. This site is approximately 100 m x 30 m and is seeded with various UXO and clutter targets (Nelson et al. 1998). The field is relatively flat and grass covered. The dual-sensor system was deployed in a hand-held configuration with the magnetometer offset ahead of the center of the EM coil assembly by 0.07 m relative to the direction of travel (Figure 13).

Test site navigation was performed using flags positioned along the area parallel to the intended survey line direction. The flags were spaced at 2-m intervals and the sensor line spacing was 0.5 m. Relative positioning of the data was accomplished using the ArcSecond positioning system. In this implementation, four transmitter beacons were used. The data collection was delayed by one day due to snowfall, which caused a reduction in the range of the beacons.

During the course of the survey a number of technical issues arose. The most serious of these issues was the failure of the magnetometer shortly after the start of the survey. This problem was later traced to electronic noise introduced by the magnetometer power supply. In an effort to

lengthen the battery life of the GEM-3 sensor, power was supplied to the GEM-3 in parallel with that supplied to the magnetometer. When the internal GEM-3 battery became slightly depleted, the charging circuitry in the GEM-3 was activated in a manner that caused noise in the power supply and resulted in the failure of the magnetometer.



Figure 13. Dual-sensor system deployed in a hand-held configuration at Blossom Point UXO Test Site, MD.

Dynamic survey findings

The survey data were positioned and presented in color grid format for review as shown in Figures 14 and 15. Visual inspection of these data show the complementary nature of the two sensor technologies. For example, target D-15 is detected with the EM sensor but has a very small signature in the magnetic data set. Conversely target E-14 presents a very strong magnetic anomaly but has a very weak EM response.

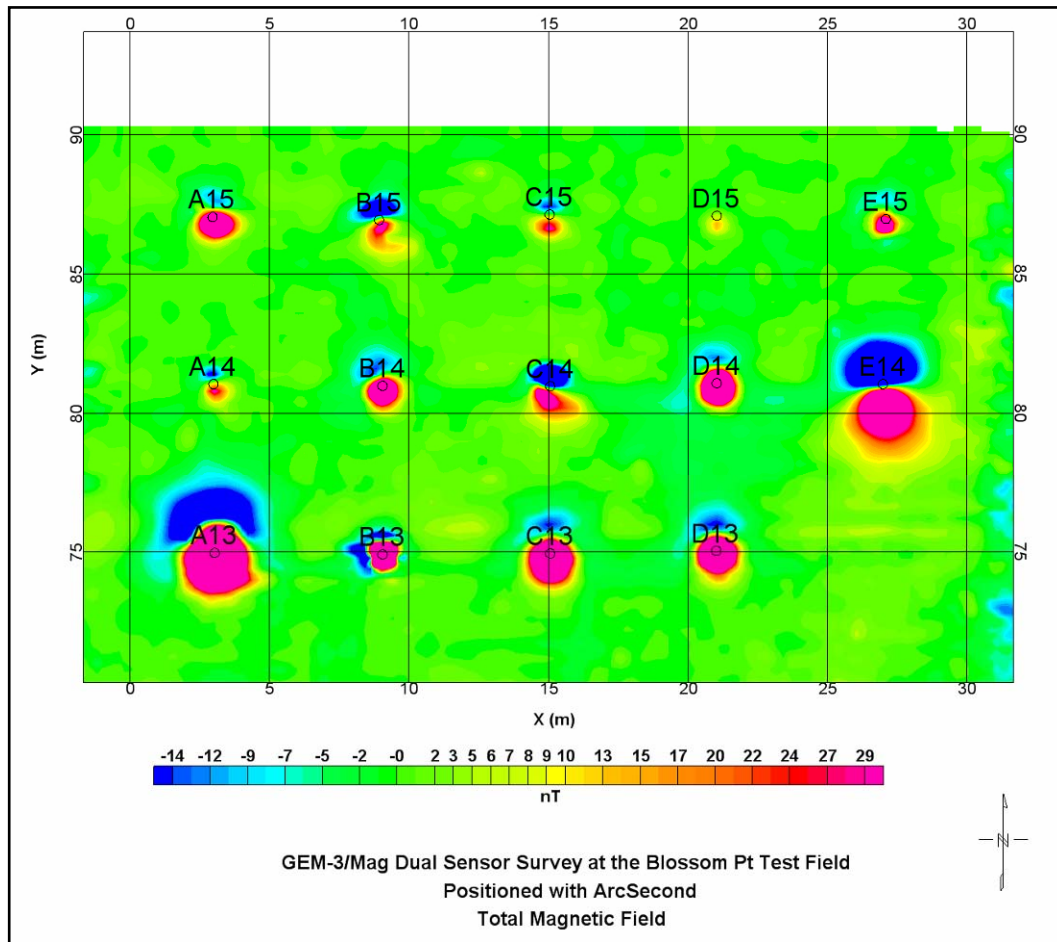


Figure 14. Total magnetic field data collected at the Blossom Point UXO Test Site.

The signal-to-noise ratios (SNRs) for each target were calculated as:

$$SNR(dB) = 10 \log_{10} \left(\frac{\sum S^2}{n} \right) \quad (3)$$

where values for S are retrieved from a localized sample of data observed to be exhibiting an anomalous response over the target and values for n are retrieved from a similar (with respect to sample size) set of data collected over a non-anomalous area. For the EM data, the sum of the Quadrature channels was used for detection and calculation of the target SNRs. Due to the structured nature of a magnetic total field dipolar response, the magnetic analytic signal was used for these calculations.

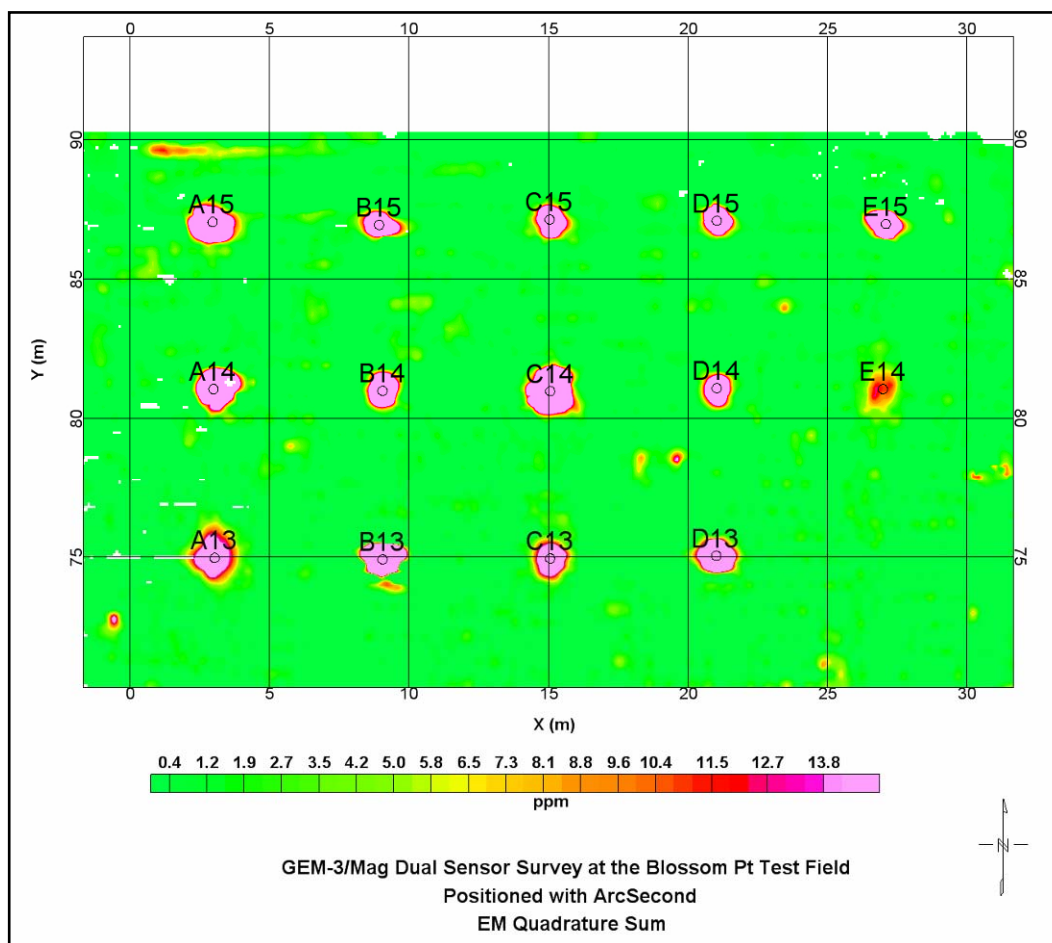


Figure 15. EM quadrature sum data collected at the Blossom Point UXO Test Site.

Using this definition of SNR, it was empirically determined that a threshold of 10 dB was required for reliable detection of the emplaced targets. Figure 16 shows the SNR results for each sensing technology over a selection of emplaced targets at Blossom Point. Figure 17 compares the SNR of the GEM-3 sensor with that of the EM73, noting that the SNR for the GEM-3 data was, for most targets, slightly higher than that of the EM73.

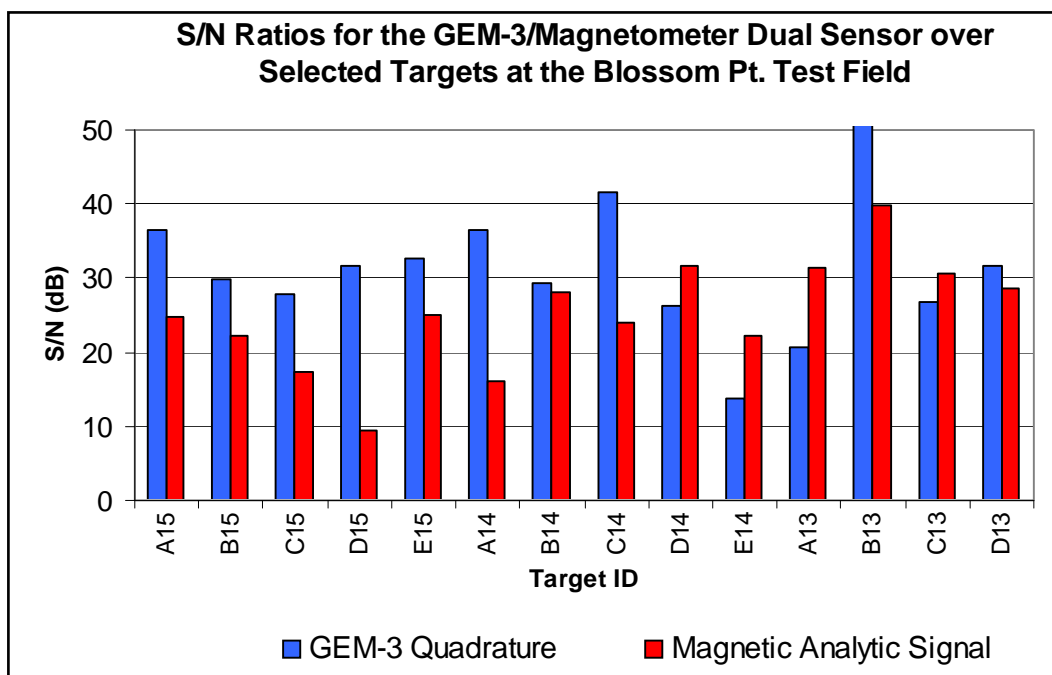


Figure 16. SNRs for dual-sensor data collected at the Blossom Point UXO test site.

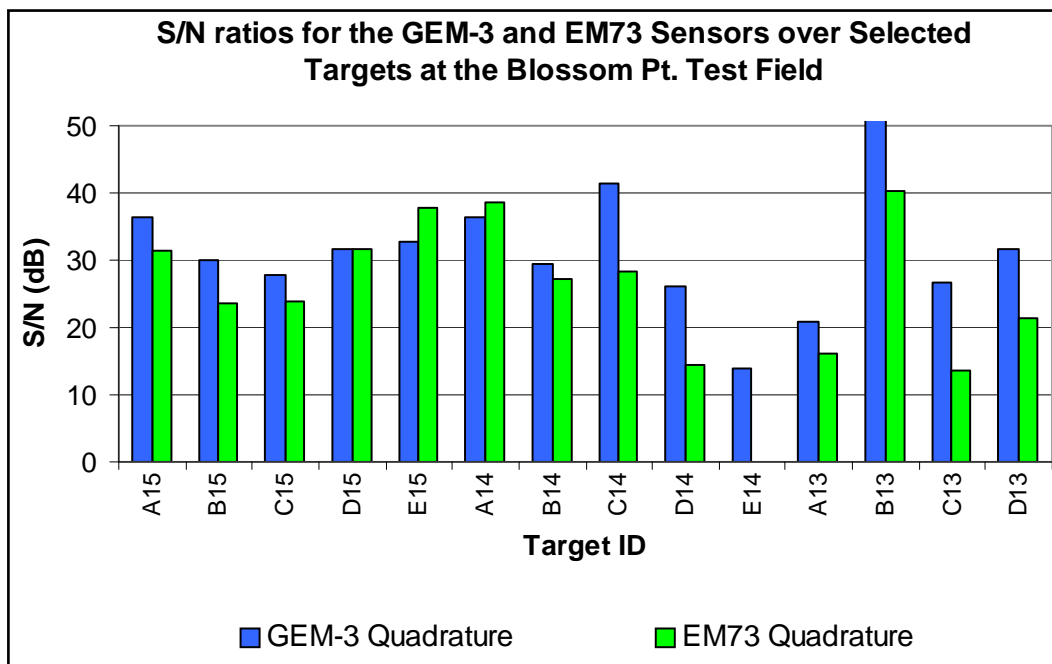


Figure 17. Comparison of GEM-3 and EM73 SNRs over selected targets at Blossom Point UXO Test Site.

The raw position data exhibited significant noise levels. The primary cause of this noise was determined to be movement of the array of positioning detectors relative to the geophysical sensors. This noise was sufficiently high in frequency to allow for application of temporal filters to reduce the

errors. Figure 18 shows the noise in the raw position data and the result of the applied filter.

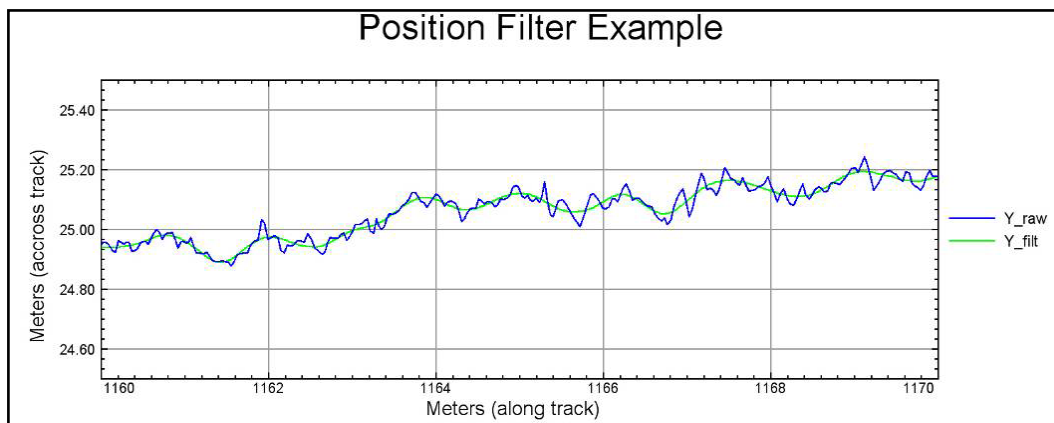


Figure 18. Raw and filtered dual-sensor position data collected using the ArcSecond positioning system.

Subsequent to the dynamic survey, the data were analyzed using the dipole fit algorithms. The imprecision of the data positioning prevents using the results of these algorithms for anything other than deriving a coarse estimate of the target positions.

Cued analysis tests

One of the goals of the shakedown test at Blossom Point was to determine the viability of using the ArcSecond system to position data collected in a cued analysis mode. Tests were performed with a UXO simulant placed in a test pit located at the Blossom Point facility. Cued analysis data were collected first using a positioning template where static measurements at predefined locations were recorded. These results were compared with measurements collected by performing repeated sweeps with the sensor being positioned with the ArcSecond system. These sweeps were performed at a number of speeds to determine the effect of accelerations on the ArcSecond positioning system. A qualitative comparison of the images shown in Figure 19 indicates that the ArcSecond system can accurately position the sensor data while the sensor is being swept back and forth as long as the sweeping motions are not inordinately fast. The errors apparent on the right hand panel are probably due as much to physical distortion of the carrying pole as to limitations of the positioning system itself. These motions were much faster than would commonly be performed during a cued investigation.

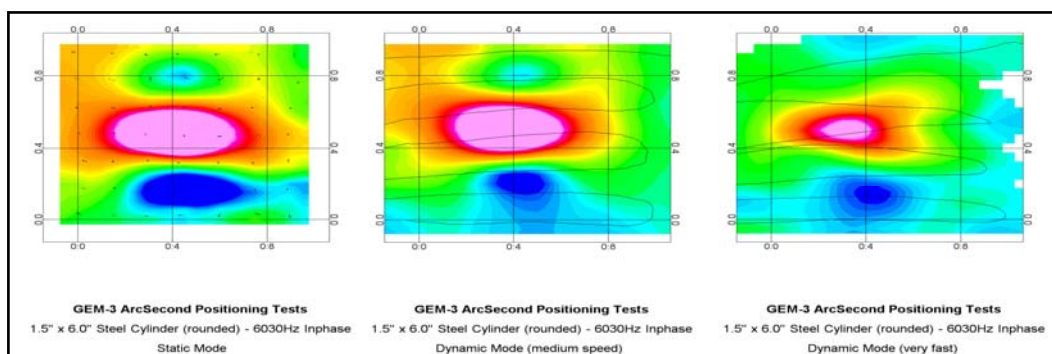


Figure 19. GEM-3 6030 Hz in-phase data collected using a template with static measurements (left panel) compared with data collected in a dynamic sweeping motion, positioned with the ArcSecond positioning system.

These sweep data were analyzed by iteratively determining the dipole model that best fit the observed data. This model is parameterized by its three dimensional position, orientation, and three orthogonal polarizability tensors (commonly called “betas”). Knowing the target response was indeed dipolar, the numeric indication of correlation between the observed data and the model then becomes a function of the quality of the sensor data, and the accuracy to which they are positioned. Thus, a quantitative measure of the effect of sweep speed on the dipole fit process can be calculated. Figure 20 shows six sweeps over a 15 cm x 4.25 cm area that were randomly sampled and submitted to the inversion analysis. The fit correlations for each set of inversions are plotted against the mean sweep speed. The fit correlations from the slow and medium sweep speeds are consistent with those obtained with static measurements using a template. The fit correlations are significantly poorer when the sweep speed becomes very high.

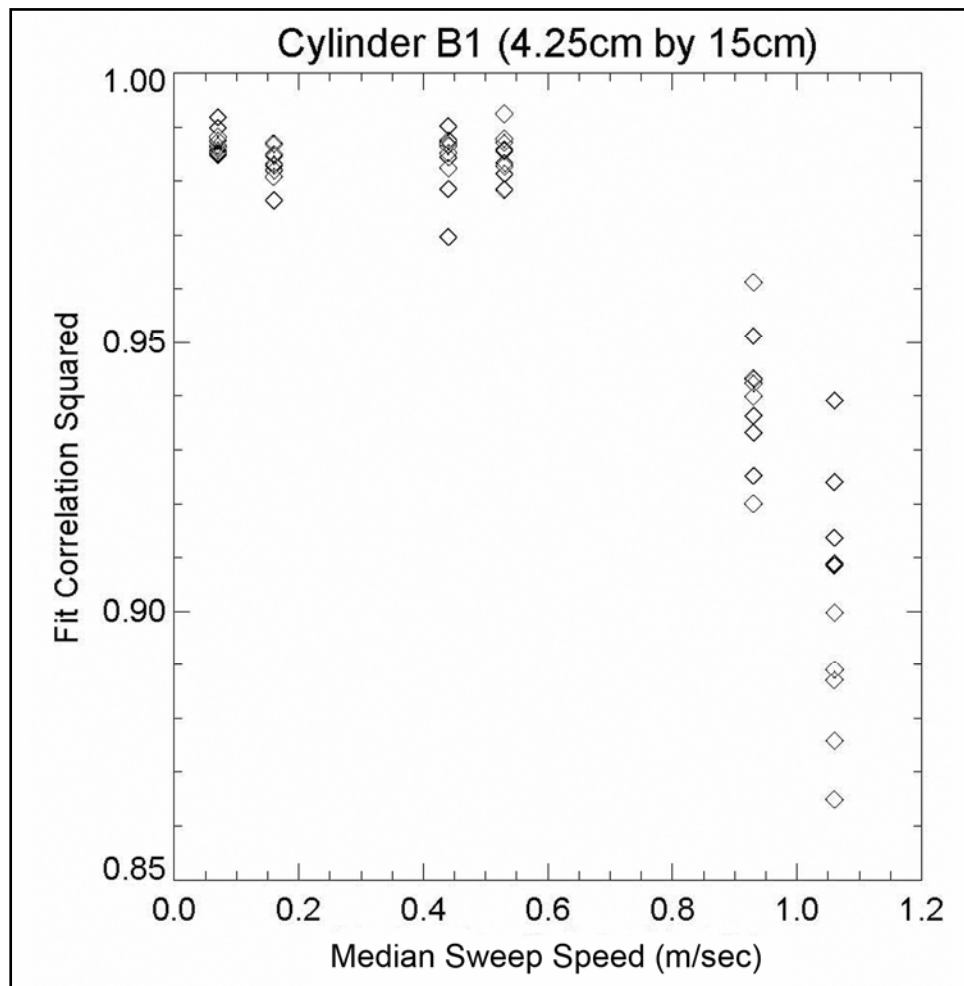


Figure 20. Quality of dipole-fit analysis as a function of sweep speed.

Field Test 2: ERDC UXO Test Site, Vicksburg, MS

The system was demonstrated at the ERDC UXO Test Site in Vicksburg, MS, during the week of 25–29 April 2005.

Site description

The ERDC UXO Test Site is at the ERDC facilities in Vicksburg, MS. The field is a 30 m x 100 m rectangle that is relatively flat and devoid of vegetation other than grass. The local geophysical environment is benign with the exception of a large metal building situated approximately 30 m south of the survey area. The test site is seeded with small to medium size UXO and clutter targets. The ground truth for these targets is known to be ambiguous with respect to the origin of the local coordinate system.

A 30 by 30 m area containing the seeded small and medium targets was surveyed using north-south lines spaced at 0.5-m intervals. The survey

data were positioned using the same ArcSecond positioning system used for the Blossom Point shakedown testing (described in the earlier “Dynamic survey test description” section), but in this test only two transmitter stations were employed.

Once again the data acquisition was curtailed due to equipment failure. In this instance the GEM-3 failed midway through the second survey day. This failure caused reasonable doubt that the positioning of the data collected on the first day was valid. The failure also occurred before significant overlap between data collected on the first and second day was accomplished. The problem was found to be that the operating software stored on an internal flash card had become corrupted. The system has since been sent to Geophex for repair and a backup flash card is now carried with the system to allow for field repairs in the case of future occurrences.

Survey results

The survey data for the small ERDC UXO block are presented in Figure 21. The EM quadrature-sum data are presented in the left panel and the total magnetic field data are shown on the right. Targets 10 through 37 are the emplaced UXO and clutter items. Unlike the previous EM73 survey, targets 15, 16, and 17 (low magnetic signature clutter items) are detected by the GEM-3 sensor. This detection is most likely due to the GEM-3 coil head having a significantly larger diameter so that the depth of penetration of this sensor is greater.

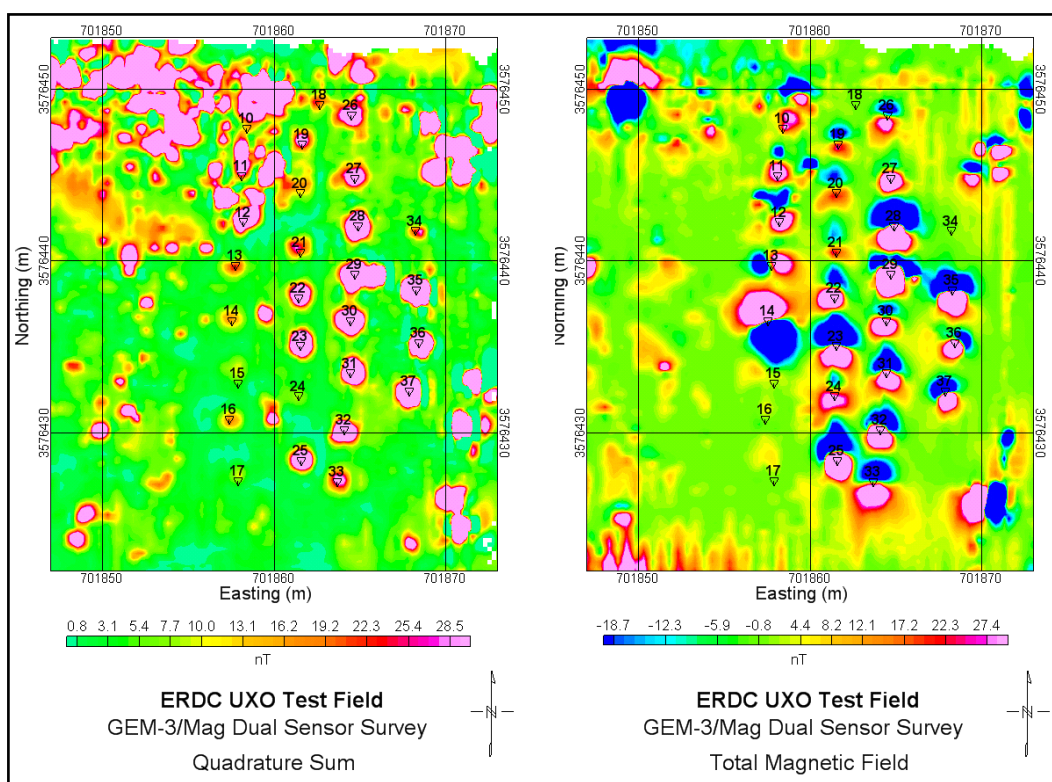


Figure 21. GEM-3 and magnetometry data collected with the dual-sensor system at the ERDC UXO Test Site.

Signal-to-noise estimates for each target were derived using the previously described methodologies. Figure 22 presents the calculated SNR for each emplaced target. Once again the complementary nature of these technologies is illustrated by the responses for targets 14 and 34.

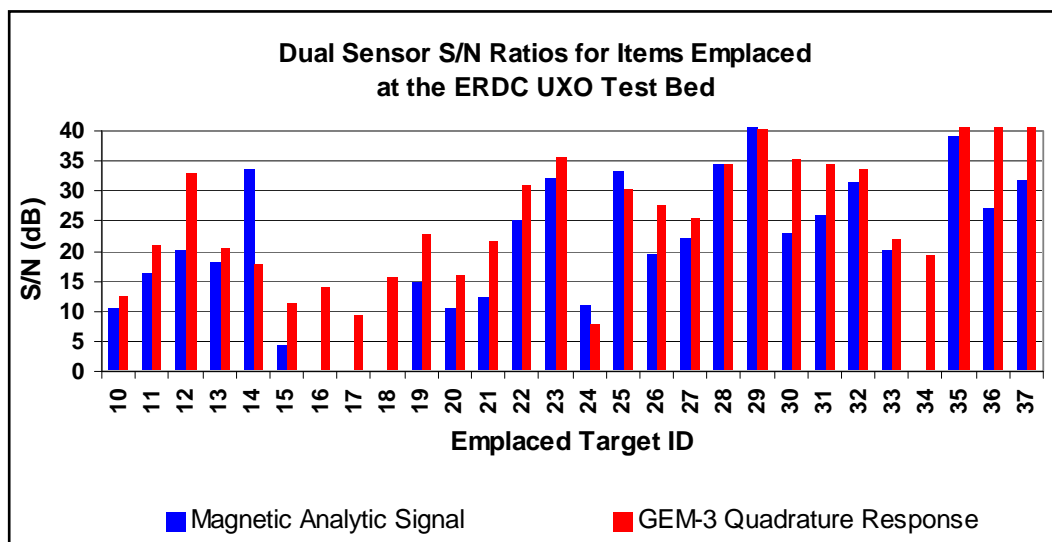


Figure 22. Dual-sensor SNR values for emplaced targets at ERDC UXO Test Site.

Field Test 3: Aberdeen Proving Ground Standardized UXO Technology Demonstration Site, MD

The multi-sensor system was deployed to the APG Standardized UXO Technology Demonstration Site from 30 May-7 July 2006. Since the hand-held dual magnetic/EMI sensor configuration was not originally designed to collect data over large areas, the system was reconfigured into a push cart setup (Figure 23) for data collection at this site.

An example of data collected at the APG Standardized UXO Technology Demonstration Site is presented in Figure 24. (No coordinates are shown on the figure in order to protect the ground truth of the APG Standardized UXO Technology Demonstration Site.) As illustrated in Figure 24, the EM data were first converted from an in-phase color scale to a gray scale. A transparent version of the magnetometer data was then overlayed onto the EM grayscale data, allowing the EM and magnetometer data to be viewed simultaneously. This method utilized the combined benefits of the EM and magnetometer data.



Figure 23. Dual-sensor system reconfigured into a push cart configuration.

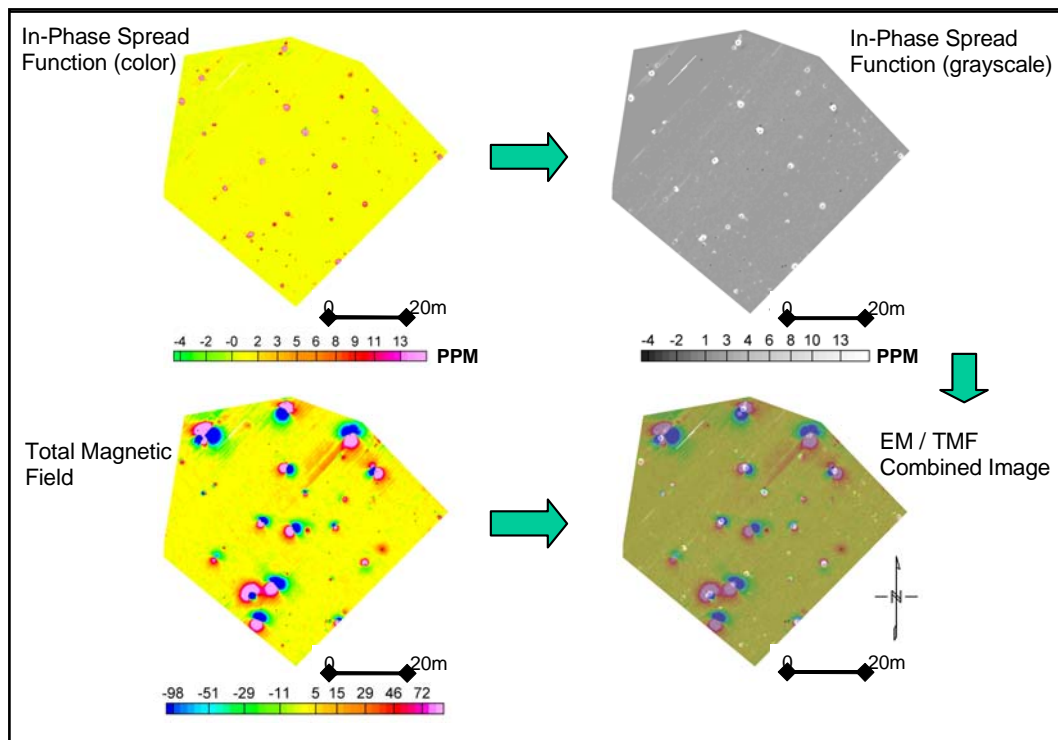


Figure 24. An example of data collected at APG Standardized UXO Technology Demonstration Site. In-phase color EM data were converted to grayscale, and then transparent magnetometer data were overlaid onto grayscale EM data.

5 Summary

The primary goal of this project was to combine a total field magnetometer with a multi-frequency EM sensor into a dual-sensor hand-held instrument for UXO detection. The steps required to successfully accomplish this goal were:

- Select a suitable multi-frequency EM sensor
- Determine an optimal magnetometer sensor position relative to the EM transmit coil
- Develop a methodology to predict and remove EM-induced offsets from the measured total magnetic field
- Design and construct suitable deployment hardware

The instrument resulting from this design process consists of sensors that are commercially available and thus can be easily duplicated with some minor mechanical and electronic engineering (for the deployment hardware, power supply, and interconnection cabling).

In addition to the design of the dual-sensor, the task of integrating the dual-sensor with the ArcSecond positioning system was performed. This integration also allows for the use of a GPS-based positioning solution.

The dual-sensor was deployed in two shakedown tests. The results of these tests confirmed that an FDEM sensor and total field magnetometer can be successfully deployed as a simultaneous, dual-sensor hand-held system.

References

- Campbell, W. H. 1997. *Introduction to geomagnetic fields*. New York, NY: Cambridge University Press.
- Nelson, H., J. McDonald, and R. Robertson. 1998. *Design and construction of the NRL baseline ordnance classification test site at Blossom Point*, NRL/MR/6110-00-8437. Washington, DC: Naval Research Laboratory.

REPORT DOCUMENTATION PAGE				<i>Form Approved</i> OMB No. 0704-0188	
<small>Public reporting burden for this collection of information is estimated to average 1 hour per response, including the time for reviewing instructions, searching existing data sources, gathering and maintaining the data needed, and completing and reviewing this collection of information. Send comments regarding this burden estimate or any other aspect of this collection of information, including suggestions for reducing this burden to Department of Defense, Washington Headquarters Services, Directorate for Information Operations and Reports (0704-0188), 1215 Jefferson Davis Highway, Suite 1204, Arlington, VA 22202-4302. Respondents should be aware that notwithstanding any other provision of law, no person shall be subject to any penalty for failing to comply with a collection of information if it does not display a currently valid OMB control number. PLEASE DO NOT RETURN YOUR FORM TO THE ABOVE ADDRESS.</small>					
1. REPORT DATE (DD-MM-YYYY) April 2008		2. REPORT TYPE Final report		3. DATES COVERED (From - To)	
4. TITLE AND SUBTITLE Multi-Sensor Systems Development for UXO Detection and Discrimination: Hand-Held Magnetic/Electromagnetic Induction Sensor				5a. CONTRACT NUMBER	
				5b. GRANT NUMBER	
				5c. PROGRAM ELEMENT NUMBER	
6. AUTHOR(S) David Wright, Hollis H. Bennett, Jr., Linda Peyman Dove, and Dwain K. Butler				5d. PROJECT NUMBER	
				5e. TASK NUMBER	
				5f. WORK UNIT NUMBER	
7. PERFORMING ORGANIZATION NAME(S) AND ADDRESS(ES) AETC Incorporated, 120 Quade Drive, Cary, NC 27513-7400; U.S. Army Engineer Research and Development Center (ERDC), Environmental Laboratory, 3909 Halls Ferry Road, Vicksburg, MS 39180-6199; Alion Science and Technology Corporation, U.S. Army Engineer Research and Development Center, 3909 Halls Ferry Road, Vicksburg, MS 39180-6199				8. PERFORMING ORGANIZATION REPORT NUMBER ERDC/EL TR-08-15	
9. SPONSORING / MONITORING AGENCY NAME(S) AND ADDRESS(ES) U.S. Army Corps of Engineers Washington, DC 20314-1000				10. SPONSOR/MONITOR'S ACRONYM(S)	
				11. SPONSOR/MONITOR'S REPORT NUMBER(S)	
12. DISTRIBUTION / AVAILABILITY STATEMENT Approved for public release; distribution is unlimited.					
13. SUPPLEMENTARY NOTES					
14. ABSTRACT The U.S. Army Engineer Research and Development Center (ERDC) in Vicksburg, MS, developed, tested, and demonstrated an innovative, hand-held, dual-sensor unexploded ordnance (UXO) detection and discrimination system. This breakthrough technology markedly reduces UXO false alarm rates by fusing two heretofore incompatible sensor platforms, integrating highly accurate spatial data in real time, and applying advanced modeling and analysis to the co-registered data stream. The ArcSecond [®] laser positioning module simultaneously integrates co-registered magnetometry and electromagnetic induction (EMI) sensor data with latitude, longitude, and elevation data at the centimeter level. This enables a vast improvement in object detection and classification in the field under a wide variety of complex geological and environmental site conditions and at sites with multiple types of military munitions. Sensor co-registration further enables major advances in physics-based modeling capabilities and applications that are unique for magnetometry and EMI sensor response. Co-registered sensors permitted the application of cooperative and joint inversion techniques that simultaneously solve both the magnetic and EM inverse problem. This approach is considerably more efficient and elegant than inverting each measurement set individually and exclusively. This breakthrough will permit the UXO remediation community to detect and discriminate 90 percent of UXO under complex site conditions, and will lead to an enormous reduction in UXO cleanup costs nationwide.					
15. SUBJECT TERMS total field magnetic, TFM, frequency domain electromagnetic (FDEM), dual magnetic/EMI sensor, unexploded ordnance (UXO), UXO test site, electromagnetic induction (EMI), EM73, G823A cesium vapor magnetometer					
16. SECURITY CLASSIFICATION OF:			17. LIMITATION OF ABSTRACT	18. NUMBER OF PAGES 45	19a. NAME OF RESPONSIBLE PERSON
A. REPORT UNCLASSIFIED	B. ABSTRACT UNCLASSIFIED	C. THIS PAGE UNCLASSIFIED			19b. TELEPHONE NUMBER (include area code)